The pH-dependent fluorescence of pyridylmethyl-4-amino-1,8-naphthalimides

A. Prasanna de Silva,* Anne Goligher, H.Q. Nimal Gunaratne, and Terence E. Rice

School of Chemistry, Queen's University, Belfast BT9 5AG, Northern Ireland
E-mail: a.desilva@qub.ac.uk

Dedicated to Professor Tony McKervey

(received 05 Mar 03; accepted 26 May 03; published on the web 30 May 03)

Abstract

Regioselective photoinduced electron transfer (PET) has been previously observed in aminoalkyl-4-amino-1,8-naphthalimide 'fluorophore-spacer-receptor' systems. PET from the amine to the fluorophore was only observed when the electron entered the fluorophore in the region of its 4-NH group. This has received two related but distinct explanations. The first is a directing effect of the molecular-scale electric field of internal charge transfer (ICT) excited state of the fluorophore. The second is a peculiarity of 4-amino-1,8-naphthalimides in possessing a node at the imide nitrogen in its frontier orbitals. The six isomeric pyridylmethyl-4-amino-1,8-naphthalimides **1**-**3** and **4**-**6** are configured as 'fluorophore-spacer-receptor' systems in order to test the relative importance of these two explanations. The two regioisomeric sets are designed such that PET is thermodynamically feasible when they are protonated, which should lead to fluorescence quenching by protons. In practice, the proton-induced fluorescence quenching is moderate and more clearly observed in the set **1**-**3**. This evidence points to the PET-accelerating effect of the molecular-scale electric field being mitigated by the presence of the node at the imide nitrogen in the frontier orbitals. Compound **4** also shows this proton-induced fluorescence quenching effect but to a still smaller extent. In this instance, the PET is hampered by the electric field alone. Compounds **5** and **6** show an excited state intramolecular proton transfer (ESIPT) involving water-mediated hydrogen-bonded rings, which dominates over any residual PET to produce proton-induced fluorescence enhancement. Again, the effect is moderate. The two mechanisms of PET regioselectivity can now be understood to operate additively in the aminoalkyl-4-amino-1,8-naphthalimides and subtractively in the protonated pyridylmethyl-4-amino-1,8-naphthalimides.

Keywords: Fluorescence, pH sensing, photoinduced electron transfer, internal charge transfer, excited state intramolecular proton transfer, molecular-scale electric field

Introduction

The photoinduced electron transfer (PET) system[1] using the 'fluorophore-spacer-receptor' format[2] is one of the most popular approaches to the design of fluorescent sensors and switches.[3,4] Aminoalkyl aromatics are perhaps the commonest examples,[5,6] with dramatic 'off-on' switching of fluorescence upon encountering the correct target. Owing to the Bronsted basicity of the amine group, these serve as fluorescent pH sensors which are finding use in physiology research.[7] In contrast, there are only a few examples which employ pyridine as the basic moiety.[8-11] These show a sharp 'on-off' switching of fluorescence upon protonation. Most of these cases however, employ aromatic hydrocarbons as fluorophores. Now we examine the use of fluorophores with push-pull π-electron systems which give rise to internal charge transfer (ICT) excited states.[12] Such states generate substantial charge separation which may influence the rate of PET processes. One system based on 1,3-diaryl-Δ^2-pyrazoline ICT fluorophores has been reported by us[8] before, but in this instance the pyridyl group was positioned almost along the bisector of the transition dipole of the ICT state so that no electric field effects were expected or seen. The previous examination of ICT fluorophores such as 4-amino-1,8-naphthalimides with aminoalkyl side-chains revealed strong regiochemical dependence of the pH-switching efficiency,[13,14] which suggested unidirectional PET processes.[13-16] PET from the amine to the fluorophore occurred only when the former was connected to the 4-amino group of the fluorophore. Unidirectional PET is most famously observed in the bacterial photosynthetic reaction centre,[17] and analogous behaviour in small molecules should permit easier analysis of the phenomenon. Current explanations focus on the influence of the excited-state electric field[13-16] and/or the effective spatial separation between the pair of orbitals involved,[18] though both these points rely on the nature of the orbitals. Therefore it was of interest to see if pyridyl analogues of these aminoalkyl-substituted fluorophores would shed further light on this issue. This issue takes on added significance given the growing body of sensors and other optical devices which employ 4-amino-1,8-naphthalimide (or closely related) fluorophores.[19-37] Hence, compounds **1**-**3** and **4**-**6** were synthesized and tested by steady-state electronic absorption and emission spectroscopy.

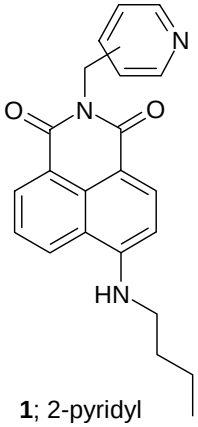

1; 2-pyridyl
2; 3-pyridyl
3; 4-pyridyl

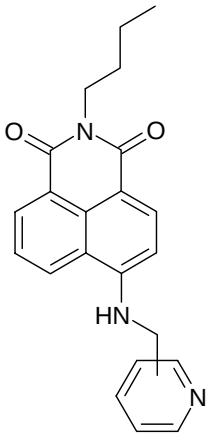

4; 2-pyridyl
5; 3-pyridyl
6; 4-pyridyl

Results and Discussion

Systems like **1** - **3** and **4** - **6** are expected to allow PET to occur from the fluorophore to the pyridine receptor when the latter is protonated. This is opposite in two ways to the situation described for 4-amino-1,8-naphthalimide fluorophores carrying aminoalkyl side-chains where PET is permitted to take place from the amine receptor to the fluorophore when the former is unprotonated.[13,14] Another contrast between the two situations is that the present cases are expected to undergo the charge shift version of PET, i.e the cationic centre moves from the pyridinium unit to the 4-amino-1,8-naphthalimide moiety. On the other hand, the aminoalkyl-substituted 4-amino-1,8-naphthalimides involve a charge separation because of PET, as may be anticipated from the electro-neutrality of the two (donor and acceptor) modules concerned. The pyridine receptor has a large decrease in its reduction potential upon protonation (–2.62 V to –1.25 V vs. sce).[38] The reduction potential of the 4-amino-1,8-naphthalimide fluorophore is measured to be –1.6 V.[39] So the PET process is thermodynamically feasible for **1** - **3** and **4** - **6** only when the pyridine receptor is protonated (ΔG_{PET} = –0.35 eV). For comparison, the ΔG_{PET} = +1.0 eV when the pyridine is proton-free. Thus we expect fluorescence to be weaker in acidic media. A frontier orbital energy picture applicable to the present cases is available in ref. 8. The receptor orbitals decrease in energy upon protonation resulting in PET becoming able to compete with fluorescence emission.

Synthesis

The synthesis of these molecules was carried out using the general synthesis of naphthalimides employed in refs. 40,41,13,14. 4-chloronaphthalic anhydride (**7**) was first reacted with each of the aminomethylpyridines separately to yield **8**, **9**, and **10** respectively. A similar reaction of **7** with n-butylamine produced **11**.[40,41,13,14,42]

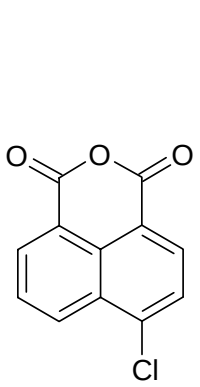

7

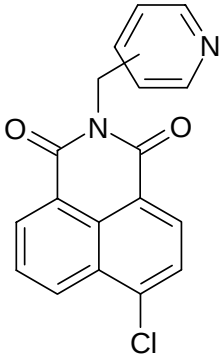

8; 2-pyridyl
9; 3-pyridyl
10; 4-pyridyl

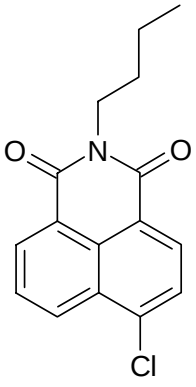

11

11 was subsequently reacted with each of the aminomethylpyridines separately to yield **4, 5** and **6**, while **8**, **9**, and **10** were reacted with n-butylamine separately to yield target molecules **1**, **2** and **3**. Each target molecule was obtained as yellow/orange solids.

Electronic spectroscopy of 1 - 3 and **4 - 6**

Electronic absorption

Electronic absorption spectroscopic measurements were carried out under conditions identical to those used for the aminoalkyl-substituted 4-amino-1,8-naphthalimides, e.g. in water:methanol (4:1, v/v) solvent.[13,14] As with these cases, absorption spectral changes of **1 - 3** and **4 - 6** upon protonation of the receptor depend on the region of the fluorophore that carries the 'spacer-receptor' assembly.

The cases with the receptor connected via the positive pole of the ICT state (4-amino position) i.e. **4 – 6** undergo a blue shift in their absorption upon protonation. This is due to repulsive interaction between the positive pole of the ICT excited state and the protonated pyridine moiety which destabilises the ICT excited state resulting in more energy being required to access the excited state (figure 1). The electron density distribution of the ICT state as deduced from calculations[43] is shown in structure **12**, which clearly indicates the positive pole of the ICT state to lie near the 4-amino position. Molecules **1 – 3** do not undergo any significant proton-induced change in absorption spectra (figure 2), as observed for other proton receptors connected via the imide position.[13,14] The diffuse negative pole of the fluorophore ICT state, which is spread over the two carbonyl groups, probably weakens any interactions. The spectral changes, where observed, can be used to calculate pK_a values from the absorbance - pH profiles shown in figure 3. Compounds **4 – 6** fit the bill as they undergo significant changes in absorbance at certain wavelengths (e.g. at 470 nm for **4**).

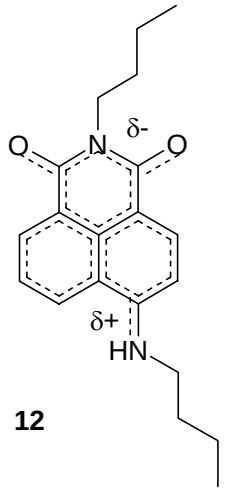

12

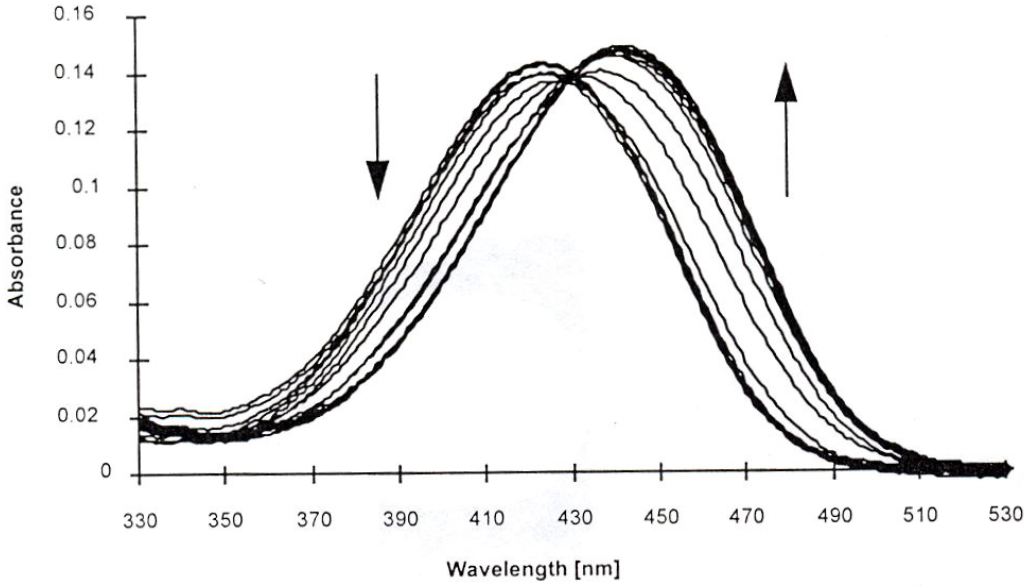

Figure 1. Family of uv-vis absorption spectra of **4** as a function of pH in water:methanol (4:1, v/v). The pH values are between 3.0 and 7.0.

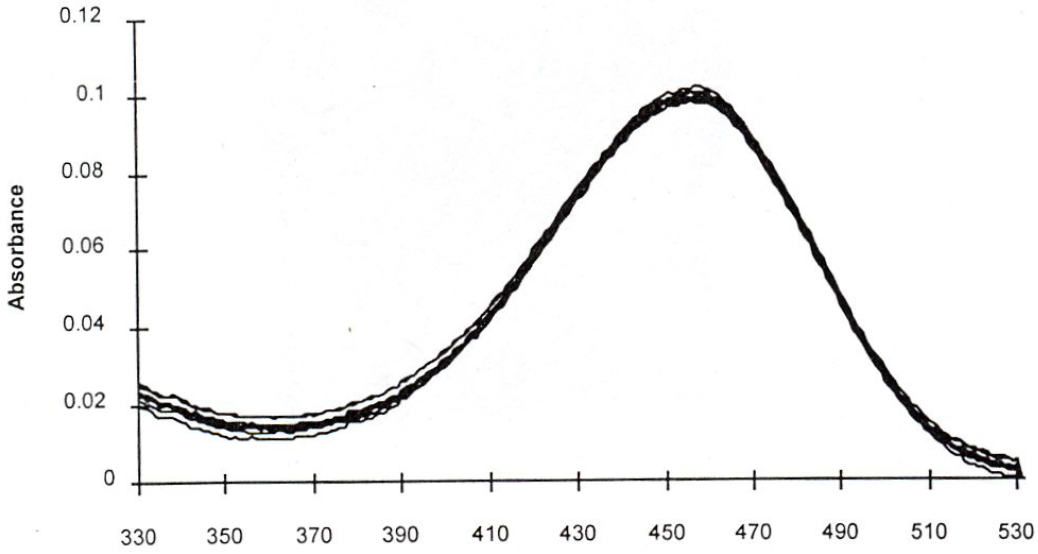

Figure 2. Family of uv-vis absorption spectra of **2** as a function of pH in water:methanol (4:1, v/v). The pH values are between 2.9 and 6.8.

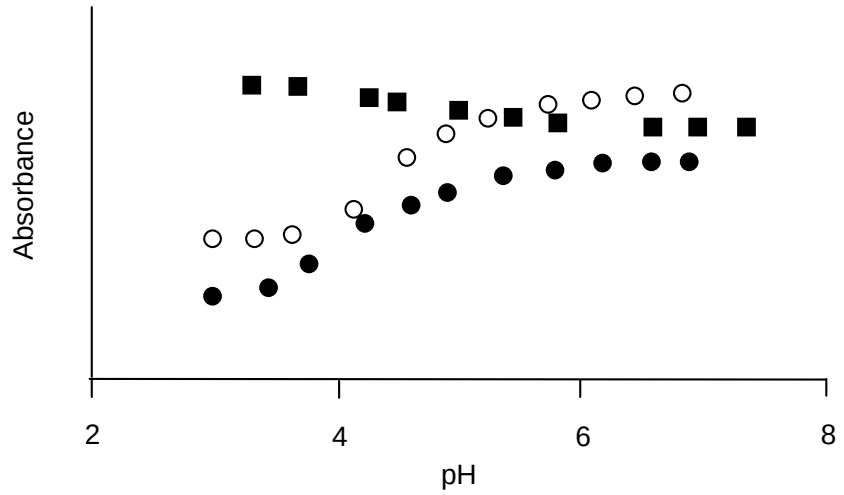

Figure 3. Absorbance - pH profiles for **4**, **5** and **6**. Open circles = **4**, measured at 470 nm, filled circles = **5**, measured at 470 nm, filled squares = **6**, measured at 420 nm.

The pK_a values obtained (Table 1) undershoot those available in the literature for 2-, 3- and 4-methylpyridines (6.0, 5.7 and 6.0 respectively),[45] because of steric inhibition to solvation of the receptor by the fluorophore and because of the electron-withdrawing nature of the nitrogen atoms of the 4-NH position. Such behaviour is common in pH-switchable PET systems.[2] The proton-induced changes in spectra, as measured by (λ_{base}-λ_{acid}) values, become less pronounced from **4** to **5** to **6** as the ICT fluorophore experiences less through-space repulsive interaction from the protonated pyridyl unit. This repulsive effect is removed in the proton-free sensors resulting in nearly identical λ_{base} values. The isosbestic wavelengths ($\lambda_{isosbestic}$) were used for excitation in the fluorescence emission experiments described later.

Table 1. Uv-vis absorption spectral parameters for **1** – **6** in water:methanol (4:1, v/v)

Parameter	**1**	**2**	**3**	**4**	**5**	**6**
$\log_{10}\varepsilon_{acid}$ $(M^{-1}cm^{-1})^a$	4.15	4.17	4.10	4.02	4.22	4.19
$\lambda_{abs.acid}$ (nm)[a]	457	458	459	424	436	439
$\lambda_{abs.base}$ (nm)[a]	458	458	458	442	443	442
$\lambda_{isisbestic}$(nm)	n/a	n/a	n/a	430	436	438
pK_a	-[b]	-[b]	-[b]	4.6[c]	4.5[c]	5.0[c]

[a] The subscripts 'acid' and 'base' refer to situations where the pyridine receptor is fully protonated and deprotonated respectively. [b] The spectral changes are too small to calculate pK_a values. [c] Obtained by analyzing absorbance - pH profiles (Figure 4) according to the equation $\log [(A_{max} - A)/(A - A_{min})] = \pm pH \pm pK_a$.[44]

Fluorescence emission

These results for the two sets of pyridyl regioisomers (**1** – **3**, and **4** – **6**) were obtained in water:methanol (4:1, v/v) as used for absorption spectroscopic experiments. pH titrations were carried out over the pH range 3.0 to 7.0 to observe any fluorescence changes over the pH range where pyridyl units undergo protonation/deprotonation.

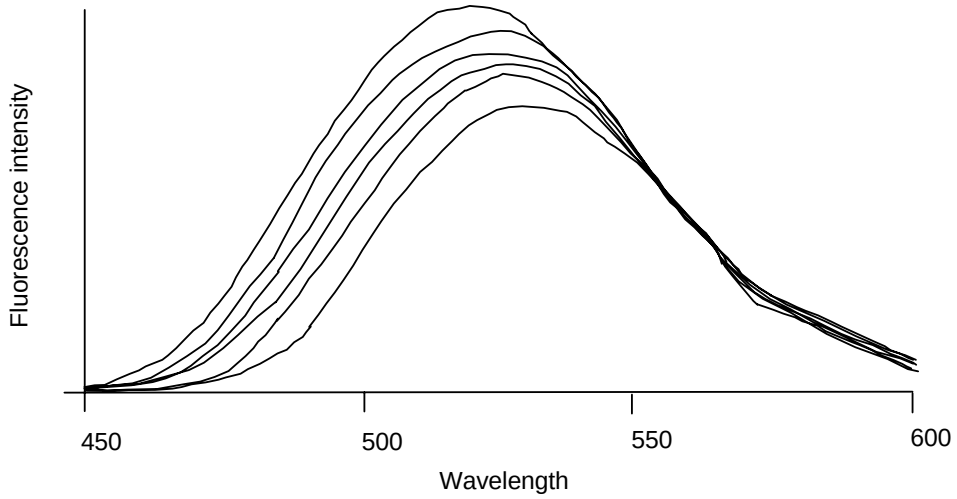

Figure 4. Family of fluorescence emission spectra of **4** as a function of pH in water:methanol (4:1, v/v). The pH values are (in order of decreasing intensity): 3.2, 3.8, 4.2, 4.6, 4.9 and 5.6.

As seen in figure 4 for **4**, the fluorescence intensity is moderately weaker in basic media which suggests that PET action from the excited state fluorophore to the protonated pyridyl moieties is absent or submerged by a different photo-process. The observed effect of fluorescence quenching in base becomes even smaller as we go from **4** to **5** to **6**. In fact **6** does show a small decrease in fluorescence on going from basic to acidic media, as shown in the quantum yield-pH plots shown in figure 5. This appears to be the extent of PET in this trio of compounds. In other words, PET to the pyridinium unit from the fluorophore does not occur when the former is connected via a methylene to the 4-amino group of the fluorophore. The electric field of the ICT state in these cases is evidently inhibiting the PET process. Hence, the fluorescence quantum yields remain substantially high (>0.22) in all three cases across the pH range.

The proton-induced blue shift in the maximum emission wavelength of **4** – **6** is caused by a repulsive interaction between the protonated pyridyl moiety and the positive pole of the ICT excited state located near the 4-amino position. Such mirroring of the proton-induced absorption spectral effect is only observed here because the basic form of **4** – **6** is still significantly emissive.

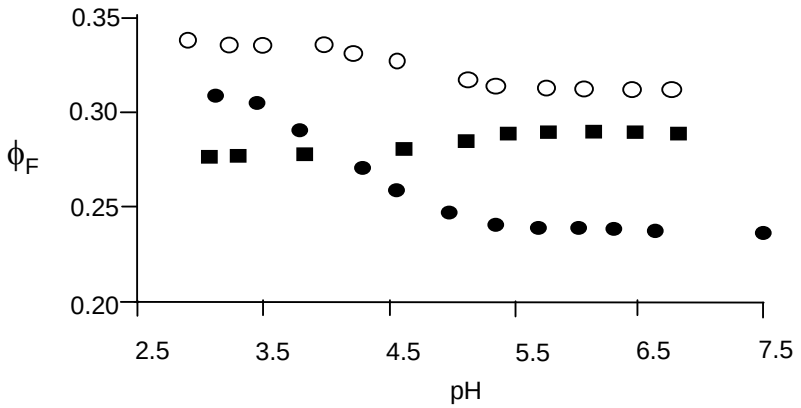

Figure 5. Fluorescence quantum yield (ϕ_F) - pH profiles for **4**, **5** and **6**. Filled circles = **4**, open circles = **5**, filled squares = **6**.

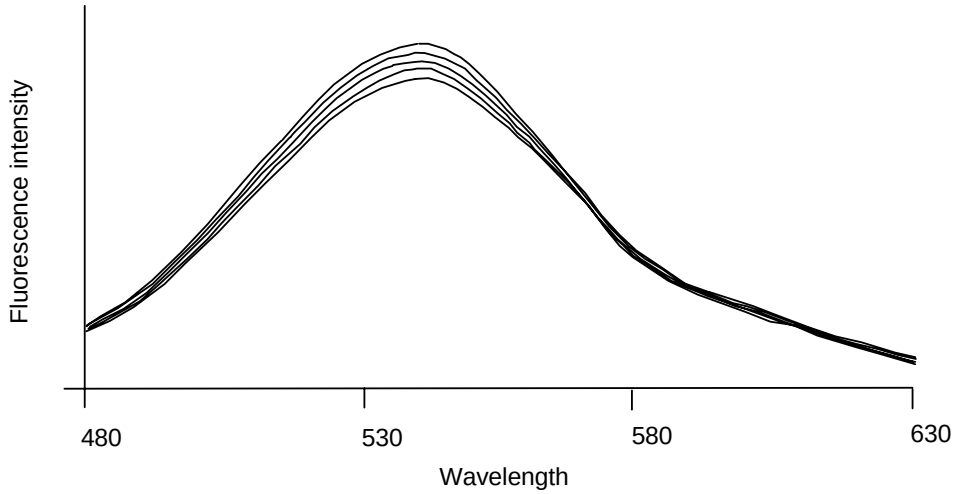

Figure 6. Family of fluorescence emission spectra of **3** as a function of pH in water:methanol (4:1, v/v). The pH values are (in order of increasing intensity): 2.8, 4.3, 4.6, 5.1 and 5.7.

The different photo-process causing fluorescence quenching of **4** and **5** in basic solution can be attributed to an excited-state intramolecular proton transfer (ESIPT) involving one or two hydrogen-bonded water molecules respectively. Naturally, such hydrogen-bonded rings of reasonable size are most probable with **4** containing the 2-pyridyl moiety and least likely with **6** based on the 4-pyridyl moiety. The positive pole of the ICT excited state located near the 4-NH group should aid the hydrogen-bond donor ability of the latter. The influence of hydrogen-bonded chains of water molecules on ESIPT has been considered before in the case of 7-hydroxy coumarin,[46] though the classic case of ESIPT is methyl salicylate where the intervention of water molecules is not necessary.[47]

Emission spectra of **3** (figure 6) show a small effect of proton-induced fluorescence quenching. Though small, this effect is significant because the 4-amino-1,8-naphthalimide fluorophore shows almost no pH-dependence of fluorescence spectra until rather extreme pH values are reached.[48] Importantly, the proton-induced fluorescence effect of **3** is now opposite to that encountered with regioisomers **4** and **5**. This fluorescence quenching can be assigned to PET

occurring from the fluorophore upon protonation of the pyridyl receptor. Again, the fluorescence quantum yields remain substantially high (>0.17) in all three cases **1** - **3** across the pH range. The fluorescence quantum yield (ϕ_F) - pH profiles for **1**, **2** and **3** are shown in figure 7. Interestingly, there is no particular bias towards the isomer containing the 2-pyridyl moiety. Ring-forming processes are therefore unlikely to contribute.

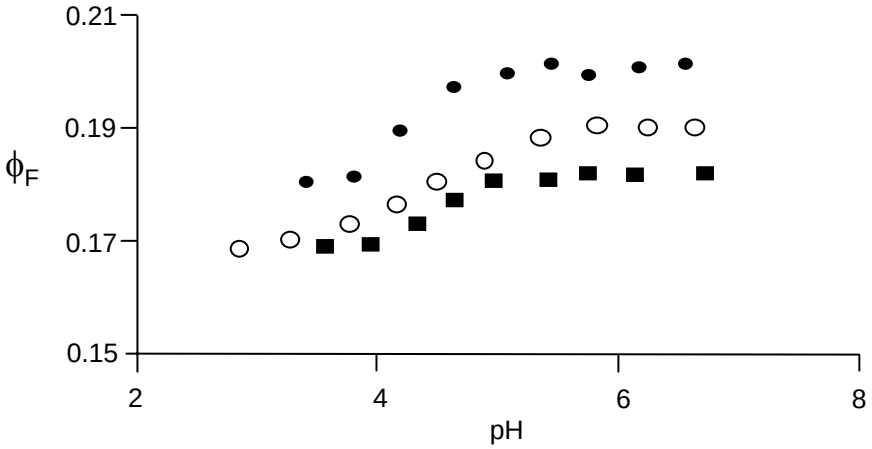

Figure 7. Fluorescence quantum yield (ϕ_F) - pH profiles for **1**, **2** and **3**. Filled squares = **1**, filled circles = **2**, open circles = **3**.

The low efficiency of PET for **1** – **3** in acid medium requires explanation. One point to consider is the fact that we do not achieve charge separation in these systems upon electron transfer from the fluorophore to the protonated pyridyl group but merely a charge shift. Most of the literature concerning fluorescent PET signalling systems[4] involves charge separation upon electron transfer. However, we note that previous examples of charge-shift PET signalling systems based on anthracene/pyridine (ΔG_{PET} = –0.7 eV) and 1,3-diaryl-Δ^2-pyrazoline/pyridine (ΔG_{PET} = –1.1 eV and + 0.1 eV) fluorophore/receptor pairs showed efficient electron transfer. The spacer modules are different from the present case in each of these instances. So the explanation does not appear to lie in factors of ΔG_{PET} or spacer length. The electric field of the ICT excited state is certainly in a direction which should favour PET action in **1** – **3** as compared to their regioisomers **4** – **6**, though the observed differences are much smaller than those seen in the aminoalkyl 4-amino-1,8-naphthalimide series.[13,14] This weakening of the electric field-induced acceleration of PET can be assigned to the nodes present at the imide nitrogen in both the frontier orbitals of 4-amino-1,8-naphthalimides.[18] Such nodes increase the effective distance over which the electron has to jump during PET. However, the formation of an intramolecular hydrogen bond between the protonated 2-pyridyl moiety and a carbonyl oxygen at the imide position of **1** to produce ESIPT cannot be ignored as an additional deactivation channel.

The fluorescence quantum yield (ϕ_F) - pH profiles can be analysed to obtain pK_a values for the pyridyl receptors. These and other parameters concerning pH-dependent emission spectra are summarized in Table 2. The pK_a values largely agree with the results obtained from absorption spectral experiments. Fluorescence enhancement (FE) factors are taken as ($\phi_{Fbase}/\phi_{Facid}$) to afford a value greater than 1 in a majority of the current cases. These can be profitably analyzed further

if we assume that the fluorescence lifetime of the 4-amino-1,8-naphthalimide fluorophore as measured for a simple di-butyl derivative,[13] is applicable to **1** – **6**. The PET rate constants (k_{PET}) calculated as detailed in Table 2, clearly show values of 1.2 – 3.3x10^7 s^{-1} for **1** – **3** whereas the corresponding value for **6** is only 0.5x10^7 s^{-1}. So the electric field influence on the PET rate in these systems results in a regioselectivity factor of 2.4 in favour of the imide side of the fluorophore. In contrast, the aminoalkyl-4-amino-1,8-naphthalimides attained a factor of >26 in favour of the 4-NH side.[13] The sides of the fluorophore which are favoured for PET are fully in line with the electric field direction. The difference in the magnitudes of these factors can be clearly attributed to the difficulty of the electron jump across the nodes at the imide nitrogen in the frontier orbitals. This effect opposes the electric field influence in the protonated pyridylalkyl-4-amino-1,8-naphthalimides. On the other hand, it acts with the electric field influence in the unprotonated aminoalkyl-4-amino-1,8-naphthalimides. The reason for these two situations of helping or hindering is simply because the PET occurs from the fluorophore towards pyridinium groups whereas PET occurs to the fluorophore from amino groups. The electric field influence on PET is necessarily vectorial, whereas the effect of the node is a scalar quantity.

Table 2. Fluorescence emission spectral parameters for **1** – **6** in water:methanol (4:1, v/v)

Parameter	**1**	**2**	**3**	**4**	**5**	**6**
$\lambda_{Flu.acid}$ (nm)[a]	537	540	539	518	523	522
$\lambda_{Flu.base}$ (nm)[a]	536	541	540	531	530	530
ϕ_{Facid}	0.17	0.18	0.17	0.31	0.34	0.27
ϕ_{Fbase}	0.18	0.20	0.19	0.24	0.31	0.28
FE ($\phi_{Fbase}/\phi_{Facid}$)	1.05	1.14	1.12	0.76	0.93	1.02
k_{PET} (10^7 s^{-1})[b]	1.2	3.3	2.9	-	-	0.5
pK_a[c]	4.7	4.4	4.7	4.5	4.4	4.6

[a] The subscripts 'acid' and 'base' refer to situations where the pyridine receptor is fully protonated and deprotonated respectively. [b] Obtained from the following relations in acidic and basic solution: $\phi_{Facid} = k_F/(k_F + k_D + k_{PET})$ and $\phi_{Fbase} = k_F/(k_F + k_D)$.[49] $\tau_F = 1/(k_F + k_D) = 4.2$ ns.[13] $k_{PET} = 0.24[(\phi_{Fbase}/\phi_{Facid}) - 1]x10^9$ s^{-1}. [c] Obtained by analyzing fluorescence quantum yield (ϕ_F) - pH profiles (Figures 5 and 7) according to the equation $\log [(\phi_{Fmax} - \phi_F)/(\phi_F - \phi_{Fmin})] = \pm pH \pm pK_a$.[44]

For completeness, the rate constants of the ESIPT process can be estimated as 7.2x10^7 s^{-1} and 2.4x10^7 s^{-1} by equations similar to those used in Table 2, footnote b. Of course, this assumes that PET processes are negligible. An estimate for the latter value, 0.5x10^7 s^{-1}, comes from **6**.

Conclusions

The charge shift PET process from the 4-amino-1,8-naphthalimide fluorophore to the protonated pyridine receptor in **4** – **6** competes moderately with fluorescence to deactivate the excited state. The moderate effect observed is due to two opposing effects. The molecular-scale electric field

of the ICT excited state accelerating the PET process in these cases and the node at the imide nitrogen in the frontier orbitals retarding electron transfer in general. Regioisomers **1** – **3** show this PET process even less due to: a) the molecular-scale electric field of the ICT excited state retarding the PET process, and b) the presence of a dominant ESIPT process in cases where a hydrogen-bonded chain connects the 4-NH group and the pyridine nitrogen. The presence of the internal electric field in the ICT excited state is further evidenced by the blue shift in the absorption and fluorescence maxima of **4** – **6** upon protonation of their respective pyridyl receptors.

Experimental Section

General Procedures. ^{1}H NMR spectra were recorded on a General Electric GN-Ω 500 (500MHz) instrument. Absorption spectra were recorded on a Perkin-Elmer Lambda 9 UV-Vis-NIR spectrometer. Fluorescence emission spectra were recorded on a Perkin-Elmer LS-5B luminescence spectrometer. Infrared spectra were recorded on a Perkin-Elmer model 983G instrument. Electrospray mass spectra were recorded on a VG Quattro II Triple Quadrupole Mass Spectrometer.

***N*-(2'-pyridylmethyl)-4-chloro-1,8-naphthalimide (8).** 2-aminomethyl pyridine (2.32g, 21.5mmol) was added to a suspension of 4-chloro-1,8-naphthalic anhydride (**7**) (5.00g, 22mmol) in toluene (100ml). The mixture was refluxed for 4 hours. Toluene was then removed under reduced pressure (0.1mmHg) at 50°C. The resulting solid was then dissolved in 1M HCl and washed with dichloromethane. The acid layer was then basified with solid sodium carbonate and extracted with dichloromethane. The dichloromethane layer was then removed under reduced pressure. The solid obtained was recrystallised from ethanol and yielded **8** as pale yellow crystals. (91% yield) m.p. 144°C-146°C. Anal. Calcd for $C_{18}H_{11}N_2O_2Cl$: C, 67.92; H, 3.45; N 8.79%. Found: C, 67.55; H, 3.33; N 8.97%. ^{1}H-NMR ($CDCl_3$) δ 5.53 (s, 2H, NC<u>H</u>$_2$Ar), 7.12-8.73 (m, 9H, Ar<u>H</u>). m/z (%): 322 (M^+,100), 305 (74), 241 (34), 187 (35), 161 (38), 108 (45). ir (KBr) ν_{max} 3468, 2919, 2851, 2346, 1772, 1738, 1717, 1672, 1582, 1022, 776cm^{-1}.

***N*-(3'-pyridylmethyl)-4-chloro-1,8-naphthalimide (9).** This was obtained using 3-aminomethyl pyridine by a similar procedure to that used in the preparation of **8**. The solid obtained was recrystallised from ethanol and yielded **9** as yellow crystals. (80% yield) m.p. 199-201°C. Anal. Calcd for $C_{18}H_{11}N_2O_2Cl$: C, 67.92; H, 3.45; N 8.79%. Found: C, 67.88; H, 3.40; N 8.65%. ^{1}H-NMR ($CDCl_3$) δ 5.31 (s, 2H, NC<u>H</u>$_2$Py), 7.15-8.77 (m, 9H, Ar<u>H</u>). m/z (%): 322 (M^+, 94), 305 (100), 214 (25), 187 (36), 161 (40), 126 (32), 108 (47). ir (KBr) ν_{max} 3468, 2910, 2853, 2346, 2298, 1702, 1694, 1656, 1597, 1364, 761cm^{-1}.

***N*-(4'-pyridylmethyl)-4-chloro-1,8-naphthalimide (10).** This was obtained using 4-aminomethyl pyridine by a procedure similar to that used in the preparation of **8**. The solid obtained was recrystallised from ethanol and yielded **10** as pale yellow crystals (56% yield) m.p. 165°C-166°C. Anal. Calcd for $C_{18}H_{11}N_2O_2Cl$: C, 67.92; H, 3.45; N 8.79%. Found: C, 67.30; H,

3.29; N 8.66%. ^{1}H-NMR ($CDCl_3$) δ_H 5.36 (s, 2H, NC$\underline{H}_2$Py), 7.40-8.69 (m, 9H, Ar$\underline{H}$). m/z (%): 322 (M^+, 100), 305 (10), 232 (56), 188 (70), 160 (47), 108 (59). ir (KBr) ν_{max} 3468, 2917, 2843, 2346, 2320, 1776, 1702, 1671, 1656, 1567, 1350, 1305, 1201, 1083, 782cm^{-1}.

***N*-(2'-pyridylmethyl)-4-butylamino-1,8-naphthalimide (1).** N-(2'-pyridylmethyl)-4-chloro-1,8-naphthalimide (**8**) (1.00g, 3.1mmol) was dissolved in n-butylamine (2.27g, 31mmol) in a stoppered boiling tube and the mixture heated for 4 hours at 100°C. The resulting dark yellow mixture was evaporated to dryness under reduced pressure (0.1mmHg) at 50°C. The resulting solid was recrystallised from ether/hexane to give **1** as yellow crystals (82% yield), m.p. 140-141°C. Anal. Calcd for $C_{22}H_{21}N_3O_2$: C, 73.54; H, 5.85; N 11.70%. Found: C, 73.49; H, 5.55; N, 11.59%. ^{1}H-NMR ($CDCl_3$) δ 0.98 (t, 3H, J-7Hz, C$\underline{H}_3$CH$_2$), 1.57 (m, 2H, CH$_3$C$\underline{H}_2$CH$_2$), 1.82 (m, 2H, CH$_3$CH$_2$C$\underline{H}_2$CH$_3$), 3.38 (m, 2H, NC$\underline{H}_2$CH$_2$) 5.35 (brs, 1H, N$\underline{H}$), 5.40 (s, 2H, NC$\underline{H}_2$Py), 6.68-8.86 (m, 9H, Ar$\underline{H}$). m/z (%): 359 (M^+, 100), 324 (61), 307 (32), 268 (33), 225 (41), 182 (93) 154 (42), 41 (52). ir (KBr) ν_{max} 3376, 2964, 2926, 2846, 1687, 1637, 1587, 1382, 1352, 1262, 1140, 1092, 1029, 867cm^{-1}.

***N*-(3'-pyridylmethyl)-4-butylamino-1,8-naphthalimide (2).** This was obtained using N-(3'-pyridylmethyl)-4-chloro-1,8-naphthalimide (**9**) by a procedure similar to that used in the preparation of **1**. The resulting solid was recrystallised from ether/hexane to give **2** as yellow/orange crystals (66% yield), m.p. 167-170°C. Anal. Calcd for $C_{22}H_{21}N_3O_2$: C, 73.54; H, 5.85; N 11.70%. Found: C, 73.19, H, 5.64, N 11.53%. ^{1}H-NMR ($CDCl_3$) δ 1.03 (t, 3H, J-7Hz, C$\underline{H}_3$CH$_2$), 1.54 (m, 2H, CH$_3$CH$_2$CH$_2$), 1.79 (m, 2H, CH$_3$CH$_2$C$\underline{H}_2$), 3.41 (m, 2H, NC$\underline{H}_2$CH$_2$) 5.30 (brs, 1h, N$\underline{H}$), 5.37 (s, 2H, NCH$_2$Py), 6.72-8.83 (m, 9H, Ar$\underline{H}$). m/z (%): 359 (M^+, 100), 342 (30), 324 (33), 316 (58), 225 (21), 182 (87) 73 (37). ir (KBr) ν_{max} 3450, 2957, 2904, 2346, 2305, 1670, 1632, 1584, 1545, 1417, 1378, 1262, 1075, 802cm^{-1}.

***N*-(4'-pyridylmethyl)-4-butylamino-1,8-naphthalimide (3).** This was obtained using N-(4'-pyridylmethyl)-4-chloro-1,8-naphthalimide (**10**) by a procedure similar to that used in the preparation of **1**. The resulting solid was recrystallised from ether/hexane to give **3** as yellow/orange crystals (32% yield), m.p. 200-201°C. Accurate mass. Calcd for $C_{22}H_{21}N_3O_2$: 359.1634. Found: 359.1621. ^{1}H-NMR ($CDCl_3$) δ 1.03 (t, 3H, J=7Hz, C$\underline{H}_3$CH$_2$), 1.57 (m, 2H, CH$_3$C$\underline{H}_2$CH$_2$), 1.57 (m, 2H, CH$_3$CH$_2$C$\underline{H}_2$CH$_2$), 3.43 (m, 2H, NC$\underline{H}_2$CH$_2$) 5.32 (brs, 1H, N$\underline{H}$), 5.36 (s, 2H, NC$\underline{H}_2$Py), 6.74-8.62 (m, 9H, Ar$\underline{H}$). m/z (%): 359 (M^+, 100), 342 (67), 324 (36), 225 (21), 182 (79). ir (KBr) ν_{max} 3457, 2966, 2927, 2868, 2360, 2339, 2309, 1263, 1114, 1021, 793cm^{-1}.

***N*-butyl-4-(2'-pyridylmethylamino)-1,8-naphthalimide (4).** N-butylamine (1.57g, 21.5mmol) was added to a suspension of 4-chloro-1,8-naphthalic anhydride (**7**) (5.00g, 21.5 mmol) in toluene (100ml). The mixture was refluxed for 4 hours and the toluene was then removed under reduced pressure (0.1mmHg) at 50°C. The resulting solid was recrystallised from ethanol. This solid (**11**)(1.00g, 3.5mmol) was dissolved in 2-pyridylmethyl amine (3.78g, 35mmol) in a stoppered boiling tube and the mixture heated for 4 hours at 100°C. The resulting dark yellow mixture was evaporated to dryness under reduced pressure (0.1mmHg) at 70°C. The resulting solid was recrystallised from ether/hexane to give **4** as yellow crystals (48% yield), m.p. 159-160°C. Accurate mass. Calcd for $C_{22}H_{21}N_3O_2$: 359.1634. Found: 359.1629. ^{1}H-NMR ($CDCl_3$) δ

0.97 (t, 3H, J=7Hz, CH_3), 1.46 (sx,, J=7Hz, CH_3CH_2), 1.71 (m, 2H, $CH_3CH_2CH_2$), 4.17 (t, 2H, J=8Hz, $NCH_2CH_2CH_2$), 4.68 (d, 2H, J=4Hz, $HNCH_2Py$), 7.20 (brs, I, N<u>H</u>) 6.72-8.65 (m, 9H, ArH). m/z (%): 359 (M^+, 100), 303 (47), 182 (22), 107 (26), 93 (42), 79 (39), 69 (38), 51 (45), 43 (33). ir (KBr) ν_{max} 3451, 2967, 2919, 2343, 1695, 1640, 1586, 1524, 769, 757cm^{-1}.

***N*-butyl-4-(3'-pyridylmethylamino)-1,8-naphthalimide (5).** This was obtained using 3-pyridylmethyl amine by a procedure similar to that used in the preparation of **4**. The resulting solid was recrystallised from ether/hexane to give **5** as yellow powder (49% yield), m.p. 159-160°C. Anal. Calcd for $C_{22}H_{21}N_3O_2$: C, 73.54; H, 5.85; N 11.70%. Found: C, 72.98; H, 6.06; N 11.87%. ^{1}H-NMR ($CDCl_3$) δ 1.02 (t, 3H, J=7Hz, CH_3), 1.47 (sx, J=7Hz, $CH_3C\underline{H}_2$), 1.75 (m, 2H, $CH_3CH_2C\underline{H}_2$), 4.16 (t, 2H, J=8Hz, $NC\underline{H}_2CH_2CH_2$), 4.71 (d, 2H, J=4Hz, $HNC\underline{H}_2Py$), 7.09 (brs, IH, N<u>H</u>) 6.70-8.69 (m, 9H, ArH). m/z (%): 359 (M^+, 100), 303 (57), 107 (36), 92 (51), 80 (20). ir (KBr) ν_{max} 3434, 3970, 2867, 2789, 1622, 1583, 1415, 1362, 1134, 1026, 798, 697cm^{-1}.

***N*-butyl-4-(4'-pyridylmethylamino)-1,8-naphthalimide (6).** This was obtained using 4-pyridylmethyl amine by a procedure similar to that used in the preparation of **4**. The resulting solid was recrystallised from ether/hexane to give **6** as yellow crystals (29% yield), m.p. 142-143°C. Accurate mass. Calcd for $C_{22}H_{21}N_3O_2$: 359.1634. Found: 359.1619. ^{1}H-NMR ($CDCl_3$) δ 0.97 (t, 3H, J=7Hz, CH_3), 1.45 (sx, J=7Hz, CH_3CH_2), 1.72 (m, 2H, $CH_3CH_2CH_2$), 4.18 (t, 2H, J=8Hz, $NC\underline{H}_2CH_2CH_2$), 4.68 (d, 2H, J=4Hz, $HNC\underline{H}_2Py$), 7.10 (brs, 1H, N<u>H</u>), 6.66-8.81 (m, 9H, ArH). m/z (%): 359 (M^+, 100), 324 (36), 182 (33), 107 (20), 80 (49). ir (KBr) ν_{max} 3439, 2956, 2914, 2848, 1609, 1526, 1262, 1093, 1023, 795, 733cm^{-1}.

Acknowledgements

We thank Dr Colin P. McCoy (School of Pharmacy, Queen's University), The Department of Employment and Learning in Northern Ireland, EPSRC and the European Union (HPRN-CT-2000-00029) for support and help. We also thank Dr Bob Sweeney (Department of Chemistry, Fairmont State College, WV, USA) for valuable comments.

References

1. Bissell, R.A.; de Silva, A.P.; Gunaratne H.Q.N.; Lynch, P.L.M., Maguire, G.E.M.; McCoy, C.P.; Sandanayake, K.R.A.S. *Top. Curr. Chem.* **1993**, *168*, 223.
2. Bissell, R.A.; de Silva, A.P.; Gunaratne, H.Q.N.; Lynch, P.L.M.; Maguire, G.E.M.; Sandanayake, K.R.A.S. *Chem. Soc. Rev.* **1992**, *21*, 187.
3. *Chemosensors of Ion and Molecule Recognition*, Czarnik, A.W., Desvergne, J.-P. Eds; Kluwer: Dordrecht, 1997.
4. de Silva, A.P.; Gunaratne, H.Q.N.; Gunnlaugsson, T.; Huxley, A.J.M.; McCoy, C.P.; Rademacher, J.T.; Rice, T.E. *Chem. Rev.* **1997**, *97*, 1515.

5. de Silva, A.P.; Rupasinghe, R.A.D.D. *J. Chem. Soc., Chem. Commun.* **1985**, 1669.
6. Czarnik, A.W. *Acc. Chem. Res*. **1994**, *27*, 302.
7. Haugland, R.P. *Handbook of Fluorescent Probes and Research Chemicals* 7th Ed., Molecular Probes, Eugene, OR, 1999.
8. de Silva, A.P.; Gunaratne, H.Q.N.; Lynch, P.L.M. *J. Chem. Soc Perkin Trans. 2* **1995**, 685.
9. de Silva, A.P.; Gunaratne, H.Q.N.; McCoy, C.P. *Chem. Commun.* **1996**, 2399.
10. de Silva, S.A.; Zavaleta, A.; Baron, D.E.; Allam, O.; Isidor, E.V.; Kashimura, N.; Percarpio, J.M. *Tetrahedron Lett.* **1997**, *38*, 2237.
11. Amendola, V.; Fabbrizzi, L.; Pallavicini, P.; Parodi, L.; Perotti, A. *J. Chem. Soc., Dalton Trans.* **1998**, 2053.
12. Valeur, B. *Molecular Fluorescence* Wiley-VCH: Weinheim, 2001.
13. de Silva, A.P.; Gunaratne, H.Q.N.; Habib-Jiwan, J.-L.; McCoy, C.P.; Rice, T.E.; Soumillion, J.-P. *Angew. Chem., Int. Ed.* **1995**, *34*, 1728.
14. de Silva, A.P.; Rice T.E. *Chem. Commun.* **1999**, 163.
15. Fox, M.A.; Galoppini, E. *J. Am. Chem. Soc.* **1997**, *119*, 5277.
16. Gosztola, D; Niemczyk, M.P.; Wasielewski, M.R. *J. Am. Chem. Soc.* **1998**, *120*, 5118.
17. *The Photosynthetic Reaction Center,* Deisenhofer, J.; Norris, J.R. Eds; Academic Press: San Diego, 1993; Vol 1, 2.
18. (a) Gao, Y.Q.; Marcus, R.A. *J. Phys. Chem. A* **2002**, *106*, 1956. (b) Sweeney, R. Personal communication.
19. Greenfield, S.R.; Svec, W.A.; Gosztola, D.J.; Wasielewski, M.R. *J. Am. Chem. Soc.* **1996**, *118*, 6767.
20. Greenfield, S.R.; Svec, W.A.; Gosztola, D.J.; Wasielewski, M.R. *New J. Chem.* **1996**, *20*, 815.
21. Hasharoni, K.; Levanon, H.; Greenfield, S.R.; Gosztola, D.J.; Svec, W.A.; Wasielewski, M.R. *J. Am. Chem. Soc.* **1996**, *118*, 10228.
22. Ni, W.J.; Su, J.H.; Chen, K.C.; Tian, H. *Chem. Lett.* **1997**, 101.
23. Ramachandram, B.; Samanta, A. *Chem. Commun.* **1997**, 1037.
24. Mitchell, K.A.; Brown, R.G.; Yuan, D.; Chang, S-C.; Utecht, R.E.; Lewis, D.E. *J. Photochem. Photobiol. A: Chem*. **1998**, *115*, 157.
25. Grabchev, I. *Dyes Pigm.* **1998**, *38*, 219.
26. de Silva, A.P.; Gunaratne, H.Q.N.; Gunnlaugsson, T. *Tetrahedron Lett.* **1998**, *39*, 5077.
27. Cosnard, F.; Wintgens, V. *Tetrahedron Lett.* **1998**, *39*, 2752.
28. Ramachandram, B.; Sankaran, N.B.; Samanta, A. *Res. Chem. Intermed.* **1999**, *25*, 843.
29. Tian, H.; Xu, T.; Zhao, Y.; Chen, K.C. *J. Chem. Soc., Perkin Trans. 2* **1999**, 545.
30. Ramachandram, B.; Saroja, G.; Sankaran, N.B.; Samanta, A. *J. Phys. Chem. B* **2000**, *104*, 11824.
31. Qian, X.; Xiao, Y. *Tetrahedron Lett.* **2002**, *43*, 2991.
32. Grabchev, I.; Qian, X.H.; Xiao, Y.; Zhang, R. *New J. Chem.* **2002**, *26*, 921.
33. Grabchev, I.; Qian, X.H.; Bojinov, V.; Xiao, Y.; Zhang, W. *Polymer* **2002**, *43*, 5731.
34. Badugu, R. *Chem. Lett*. **2002**, *106*, 5572.
35. Saha, S.; Samanta, A. *J. Phys. Chem. A* **2002**, *106*, 4763.

36. He, H.; Mortellaro, M. A.; Leiner, M. J. P.; Young, S. T.; Fraatz, R. J.; Tusa, J. K. *Anal. Chem.* **2003**, *75*, 549.
37. He, H.; Mortellaro, M. A.; Leiner, M. J. P.; Fraatz, R. J.; Tusa, J. K. *J. Am. Chem. Soc*. **2003**, *125*, 1468.
38. Siegerman, H. In *Techniques of Electroorganic Synthesis. Part II* Weinberg, N.L. Ed.; Wiley: New York, 1975; p 667.
39. McCoy, C.P. *Ph.D. Thesis*, Queen's University, Belfast, 1994.
40. Alexiou, M.S.; Tychopoulos, V.; Ghorbanian, S.; Tyman, J.H.p.; Brown, R.G.; Brittain, P.I. *J. Chem. Soc. Perkin Trans. 2* **1990**, 837.
41. Xuhong, Q.; Zhenghua, Z.; Chen, K.C. *Dyes Pigm*. **1989**, *11*, 13.
42. Daffy, L.M.; de Silva, A.P.; Gunaratne, H.Q.N.; Huber, C.; Lynch, P.L.M.; Werner, T.; Wolfbeis, O.S. *Chem. Eur. J.* **1998**, *4*, 1810.
43. Pardo, A.; Campanario, J.; Poyato, J.M.L.; Camacho, J.J.; Reyman, D.; Martin, E. *J. Mol. Struct. (Theochem)* **1988**, *166*, 463.
44. de Silva, A.P.; Gunaratne, H.Q.N.; Lynch, P.L.M.; Patty, A.J.; Spence, G.L.*J. Chem. Soc., Perkin Trans. 2* **1993**, 1611.
45. (a) Perrin, D.D. *Dissociation Constants of Organic bases in Aqueous Solution*, Butterworth: London, 1965. (b) Serjeant, E.P.; Dempsey, B. *Ionization Constants of Organic Acids in Aqueous Solution*, Pergamon: Oxford, 1979.
46. Moriya, T. *Bull. Chem. Soc. Jpn*. **1983**, *56*, 6.
47. Klopffer, W. *Adv. Photochem*. **1977**, *10*, 311.
48. Yuan, D.; Brown, R.G. *J. Chem. Res. (S)*. **1994**, 418.
49. Birks, J.B. *Photophysics of Aromatic Molecules*; Wiley: New York, 1970.